Crystal structure of fibrinogen-Aα peptide 1–23 (F8Y) bound to bovine thrombin explains why the mutation of Phe-8 to tyrosine strongly inhibits normal cleavage at Arg-16

Michael G. MALKOWSKI*[1], Philip D. MARTIN*, Susan T. LORD† and Brian F. P. EDWARDS*[2]

*Department of Biochemistry, Wayne State University, 540 E. Canfield Avenue, Detroit, MI 48201, U.S.A., and †Departments of Pathology, Curriculum in Genetics and Molecular Biology, University of North Carolina at Chapel Hill, Chapel Hill, NC 27599, U.S.A.

A peptide containing residues 1–50 of the Aα-chain of fibrinogen, expressed as a fusion peptide with β-galactosidase, is rapidly cleaved by thrombin at Arg-16, similarly to whole fibrinogen. When Phe-8, which is highly conserved, is replaced with tyrosine (F8Y), the cleavage is slowed drastically [Lord, Byrd, Hede, Wei and Colby (1990) J. Biol. Chem. **265**, 838–843]. To examine the structural basis for this result, we have determined the crystal structure of bovine thrombin complexed with a synthetic peptide containing residues 1–23 of fibrinogen Aα and the F8Y mutation. The crystals are in space group $P4_32_12$, with unit-cell dimensions of $a = 88.3$ Å (1 Å = 0.1 nm), $c = 195.5$ Å and two complexes in the asymmetric unit. The final R factor is 0.183 for 2σ data from 7.0 to 2.5 Å resolution. There is continuous density for the five residues in the P3, P2, P1, P1′ and P2′ positions of the peptide (Gly-14f to Pro-18f) at the active site of thrombin, and isolated but well-defined density for Tyr-8f at position P9 in the hydrophobic pocket of thrombin. The tyrosine residue is shifted relative to phenylalanine in the native peptide because the phenol side chain is larger and makes a novel, intrapeptide hydrogen bond with Gly-14f. Adjacent peptide residues cannot form the hydrogen bonds that stabilize the secondary structure of the native peptide. Consequently, the 'reaction' geometry at the scissile bond, eight residues from the mutation, is perturbed and the peptide is mostly uncleaved in the crystal structure.

INTRODUCTION

Thrombin (EC 3.4.21.5), a serine endoprotease that preferentially cuts after arginine and sometimes lysine residues, is both a major product and a major regulator of the clotting cascade in thrombosis and haemostasis [1,2]. Bovine α-thrombin has an A-chain of 49 residues that is linked, via a single disulphide bond, to a B-chain of 259 residues that contains the catalytic residues, His-57, Asp-102 and Ser-195. {The residue numbers for thrombin in this paper are assigned by analogy with chymotrypsin [3]. Sequential capital letters are used for thrombin residues inserted into the sequence of chymotrypsin, e.g. the five residues of the autolysis loop inserted at position 149 (Thr-149A to Glu-149E). Sequence numbers for fibrinogen are identified by the suffix f.} Structures of bovine thrombin (TBN) complexed with residues 7–16 of fibrinopeptide A (FpA7) [4] and G17ψ [5] (defined in Table 1), with hirudin [6], and with small-molecule inhibitors [7], are known. Structures have also been determined for similar complexes involving human thrombin [3,8–10].

Thrombin is more specific than other serine proteases such as trypsin because of several striking insertions in the primary structure. Thrombin binds the peptide substrate in a groove that is deeper, longer and less accessible than that of similar proteases [3]. The specificity is provided by (1) an extended, apolar binding site for hydrophobic residues on the N-terminal side of the scissile bond, (2) a specificity pocket with a strong preference for arginine, (3) subsites for small, non-polar residues immediately after the scissile bond, and (4) a strongly basic groove that binds macromolecule ligands such as fibrinogen, the thrombin receptor and hirudin at acidic residues C-terminal to the scissile bond [11].

During clotting, thrombin cleaves the two Aα-chains of fibrinogen rapidly at Arg-16f and the two Bβ-chains more slowly at Arg-14f to release FpA and FpB respectively. Active site mapping with synthetic peptide analogues and with fibrinogen–Aα_{1-50} fusion proteins has shown that the first six residues of FpA do not affect the activity, whereas Asp-7f, Phe-8f, Gly-12f, Gly-13f, Val-15f and Arg-16f are required for maximal activity [12–15]. These residues occupy respectively the P10, P9, P5, P4, P2 and P1 positions of the substrate (Table 1).

Phe-8f, which triples k_{cat}/K_m when added to a synthetic peptide, is unusually important given its distance from the scissile bond [16]. An explanation for this anomaly is apparent in the three-dimensional structure of the complex of FpA7 with thrombin, in which the first five residues, Asp-7f to Glu-11f, form a turn of α-helix that brings Phe-8f back into the active site, where it lies in a hydrophobic cage next to Val-15f [4,5,10,17]. This interaction is critical. When Phe-8f is replaced with tyrosine in a fusion protein containing residues 1–50 of the Aα-chain, the fusion protein changes from being an excellent substrate to being an excellent inhibitor [12]. This surprising transformation cannot be due to a simple disruption of the α-helical turn. With a disordered N-terminus, the peptide should still bind using merely the immediate residues around the scissile bond, in the same fashion as short fibrinopeptides which are cleaved [18].

To understand these observations, we have synthesized the first 23 residues of the Aα-chain – with a tyrosine residue

Abbreviations used: Fp, fibrinopeptide; RMS, root mean square; TBN; bovine thrombin.

[1] Present address: Department of Biochemistry, Michigan State University, East Lansing, MI 48824-1319, U.S.A.

[2] To whom correspondence should be addressed.

The coordinates reported in this paper have been deposited in the Protein Data Bank and assigned the accession code 1YCP.

Table 1 Sequences (one-letter amino acid codes) and nomenclature for fibrinogen Aα peptides

The 'P' nomenclature is from [37]. Sn and Sn′ are used for the subsites on thrombin that bind the Pn and Pn′ substrate residues. A blank in the table indicates the residue is not part of the peptide. A bullet point indicates that the residue is the same as in F8Y. FpA7, G17ψ and G12V have an acetylated N-terminus. ψ denotes psuedoglycine with -CH_2- replacing the -NH- group.

Residue	1	2	3	4	5	6	7	8	9	10	11	12	13	14	15	16	17	18	19	20	21	22	23
'P' no.	16	15	14	13	12	11	10	9	8	7	6	5	4	3	2	1	1′	2′	3′	4′	5′	6′	7′
F8Y	A	D	S	G	E	G	D	Y	L	A	E	G	G	G	V	R	G	P	R	V	V	E	R
FpA7							●	F	●	●	●	●	●	●	●	●							
7ψ							●	F	●	●	●	●	●	●	●	●	ψ	●	●				
G12V							●	F	●	●	●	V	●	●	●	●							

replacing Phe-8f (peptide F8Y; Table 1) – and co-crystallized the peptide with TBN. We find that this variant peptide is not cleaved by human α-thrombin in solution or by bovine α-thrombin in the crystal.

MATERIALS AND METHODS

Preparation of proteins

TBN was prepared as described previously [19] and had between 1500 and 2000 NIH units per mg of protein. The protein was stored at −80 ° C in ammonium phosphate buffer, pH 6.5. The F8Y peptide, corresponding to N-terminal residues 1–23 of the fibrinogen Aα-chain (Table 1), with Phe-8 mutated to tyrosine, was synthesized by the protein chemistry facility of UNCCH/NIEHS, and was more than 90 % pure as assessed by HPLC.

HPLC and mass spectrometric analysis

To determine whether this peptide is a substrate for thrombin, the peptide in 50 mM Tris/HCl (pH 7.4)/150 mM NaCl at 1.8 μM final concentration was incubated with or without 9 units/ml human α-thrombin at 37 °C for 120 min. The samples were then heated at 100 °C for 2 min to stop the reaction, and centrifuged. Aliquots of each supernatant were loaded on a reverse-phase HPLC C_{18} column with buffer A (25 mM sodium phosphate, pH 6.0) and eluted with a linear gradient of buffer B [50 mM sodium phosphate (pH 6.0)/50 % (v/v) acetonitrile] as previously described [20]. HPLC tracings after 120 min at 37 °C with or without thrombin showed no cleavage of the peptide (Figure 1). Matrix-assisted laser desorption ionization MS (MALDI-MS) was performed by the Protein and Carbohydrate Structure Facility (University of Michigan, Ann Arbor, MI, U.S.A.) on protein crystals that had been isolated, collected and dissolved in 50 % (v/v) acetonitrile in distilled water.

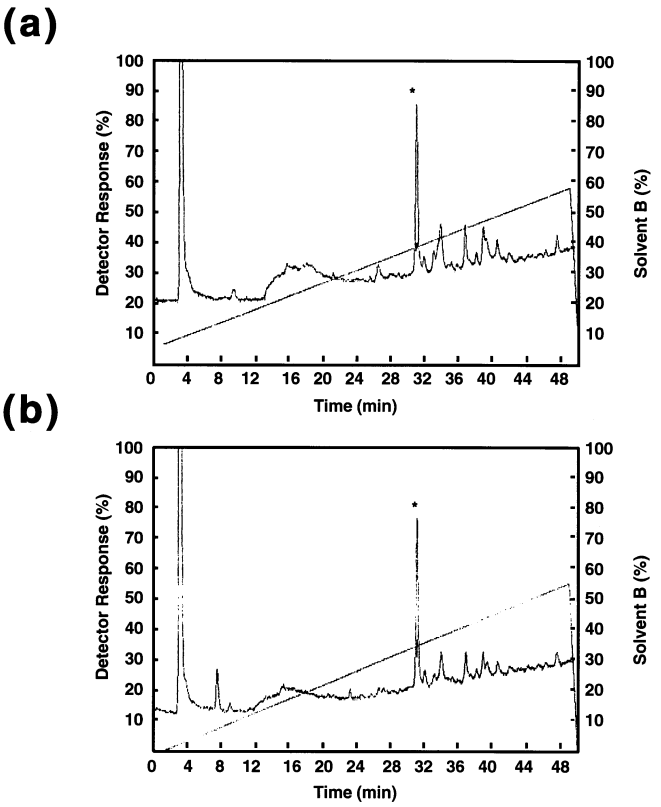

Figure 1 HPLC elution profiles

The F8Y peptide at 1.8 μM was incubated (**a**) alone and (**b**) with 9 units of human thrombin for 120 min and then analysed by HPLC on a C_{18} column as described in the text. Thrombin was eluted at approx. 8% buffer B whereas F8Y was eluted at approx. 32% buffer B.

Crystallization

The TBN–F8Y complex was prepared by mixing the peptide at a final concentration of 5 mM with a 0.4 mM solution (15 mg/ml) of TBN in 0.25 M ammonium phosphate, pH 6.0. The crystals used for data collection appeared in hanging drops equilibrated at room temperature against 2 M $(NH_4)_2SO_4$/0.1M Hepes (pH 7.5)/2 % PEG400 for 7 days and were harvested after 12 days.

Data collection

Diffraction data were collected at room temperature on two crystals of the F8Y complex (1.1 mm × 0.3 mm × 0.3 mm and 0.6 mm × 0.2 mm × 0.2 mm; 5 days old) mounted in quartz capillaries by using a Siemens area detector with a Rigaku RU200H rotating-anode X-ray source (40 kV, 70 mA) and a Supper graphite monochromator (CuKα radiation). The data collection, which was organized with the program ASTRO [21], was done at four different fixed ϕ values; a total of 880 frames, each 0.25 ° in ω, were collected. The data from the two crystals, which were scaled and merged separately with the program XENGEN [22], had R_{sym} values of 0.052 and 0.081 respectively, and an overall R_{merge} of 0.109 for 18614 unique reflections when the two separate data sets were combined by using the DIFCOR program in the ROCKS suite of programs [23]. The combined

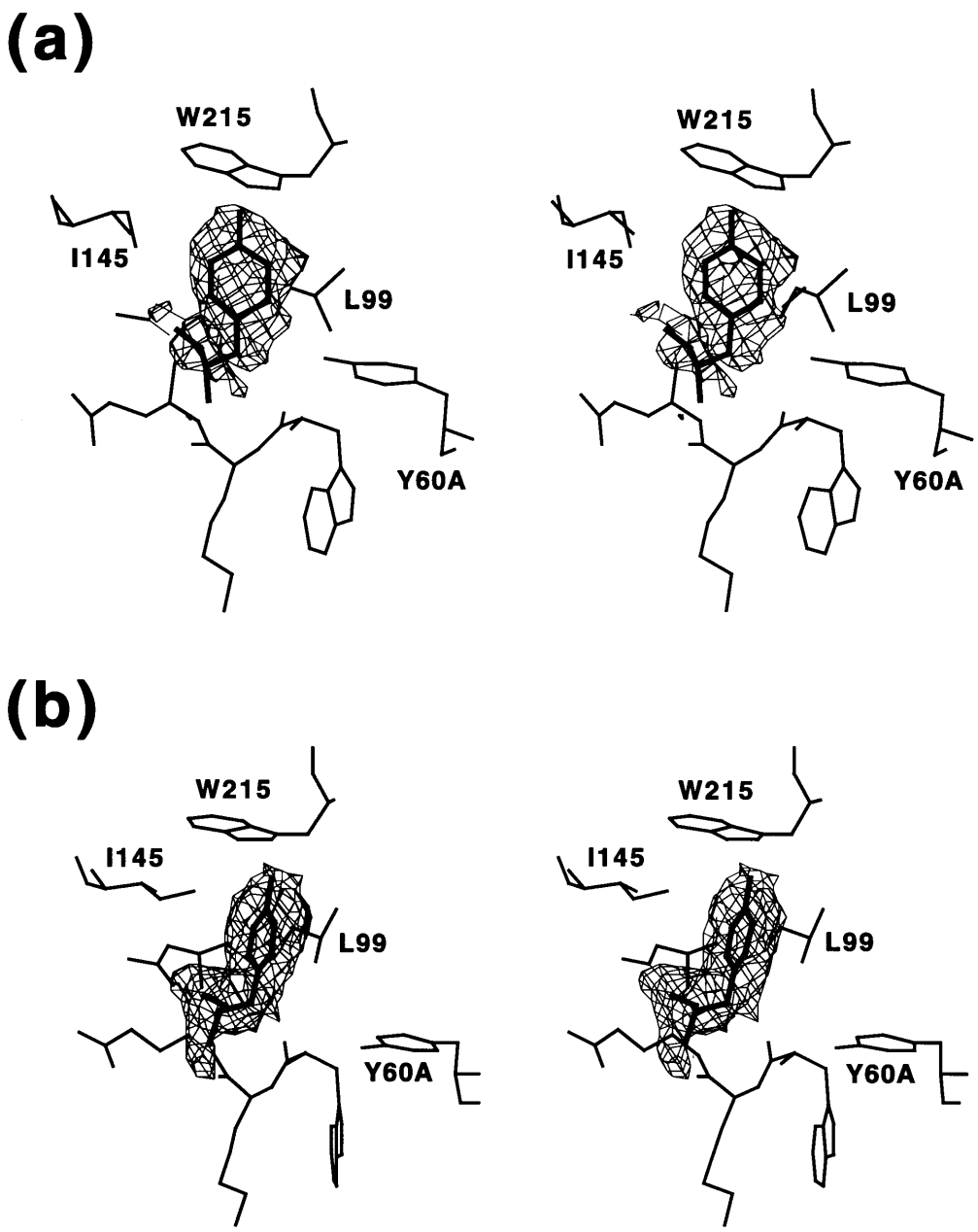

Figure 2 The electron density for Tyr-8f

Tyr-8f (thick lines), and its $2F_o-F_c$ 'omit' electron density contoured at 0.8σ are shown in stereo for (**a**) complex I and (**b**) complex II. Thrombin residues Tyr-60A, Trp-96, Leu-99, Ile-145 and Trp-215, which form a hydrophobic pocket, are shown in thin lines.

data set had an overall completeness of 63 % for data from 7.0 to 2.5 Å (1 Å = 0.1 nm) resolution (25 % complete at 2.6–2.5 Å resolution) in the last shell.

Structure solution

Crystals of the TBN–F8Y[2] complex are in space group $P4_32_12$ ($a = b = 88.3$ Å, $c = 195.5$ Å) and are isomorphous with those of TBN complexed with the G12V fibrinopeptide (Table 1), which were solved before this project by molecular replacement (P. D. Martin, M. Malkowski and B. Edwards, unpublished work) by using XPLOR [24] and TBN [4] as the model. Those calculations established the space group to be $P4_32_12$ with two crystallographically independent TBN–G12V complexes in the asymmetric unit oriented almost identically (thrombin I at $\theta_1 = 162.0°$, $\theta_2 = 77.5°$, $\theta_3 = 83.3°$; thrombin II at $\theta_1 = 163.4°$, $\theta_2 = 78.5°$, $\theta_3 = 75.2°$) and separated by approx. 0.5 of the c-axis.

This rather unusual arrangement was verified by an 'omit' map and by 'difference' molecular replacement. A $2F_o-F_c$ electron density map calculated with phases from thrombin in complex I alone and improved with SQUASH [25] showed long stretches of main-chain density that fitted the β-sheet and α-helical sections of thrombin in complex II. When the electron density for the known thrombin molecule in this $2F_o-F_c$ map was

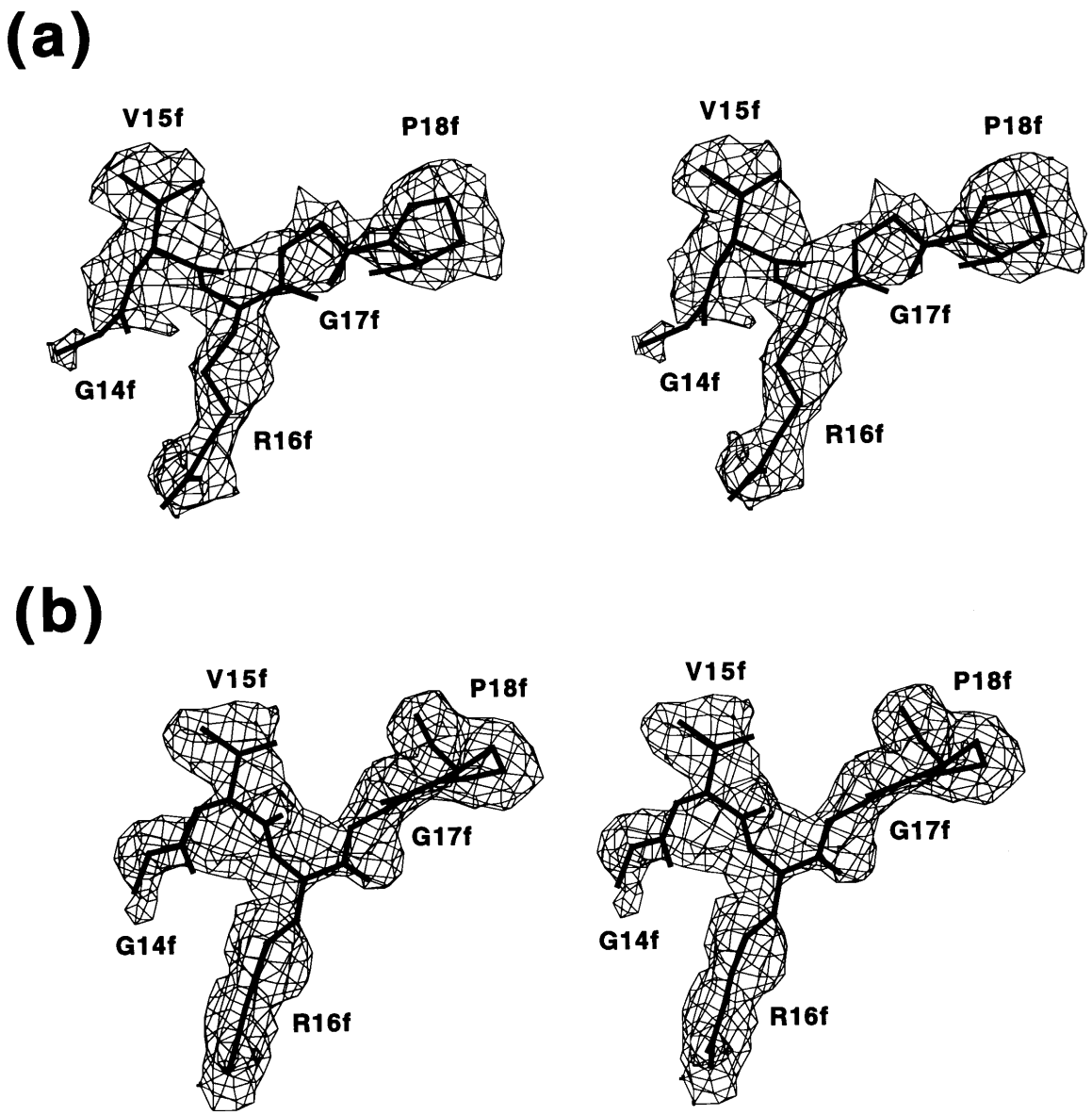

Figure 3 F8Y residues at the active site

Residues Gly-14f to Pro-18f (thick lines) are shown in stereo with the $2F_o-F_c$ 'omit' electron density calculated in XPLOR. The electron density is contoured at 0.8σ for (**a**) complex I and (**b**) complex II. The scissile bond, between Arg-16f and Gly-17f, is mostly intact as shown by the continuous electron density throughout the peptide. Thrombin residues have been left out for clarity.

zeroed and the modified map back-transformed to produce a new set of structure factors, molecular replacement calculations gave a strong solution for thrombin II. This method of subtractive molecular replacement and modifications to it have proved useful in solving other thrombin crystals with multiple complexes in the asymmetric unit [26].

Structural analysis

The coordinates for the crystal structures of human PPACK-thrombin (entry 1PPB), TBN complexed with FpA residues 7–16 (TBN–FpA7; entry 1BBR) TBN complexed with FpA residues 7–19, with a non-cleavable scissile bond (TBN–G17y; entry 1UCY), and *Streptomyces griseus* protease B complexed with turkey ovomucoid inhibitor (entry 3SGB) were obtained from the Protein Data Bank [27]. Hydrogen bonds were calculated with the program QUANTA (Molecular Simulations, San Diego, CA, U.S.A.). The criteria for a hydrogen bond are that the three angles C=O···H, O···H–N, and H–N–C be greater than 90° and the distance N···O not exceed 3.3 Å for a 'short' hydrogen bond and 4.0 Å for a 'long' one [28]. Superposition of coordinates between structures was done with the program ALIGN [29] and the Cα coordinates of the thrombin residues unless stated otherwise. 'Omit' maps were calculated in XPLOR.

RESULTS

Refinement

The refinement began with two thrombin molecules in the asymmetric unit, each with 36 A-chain residues (1H–15) and 259

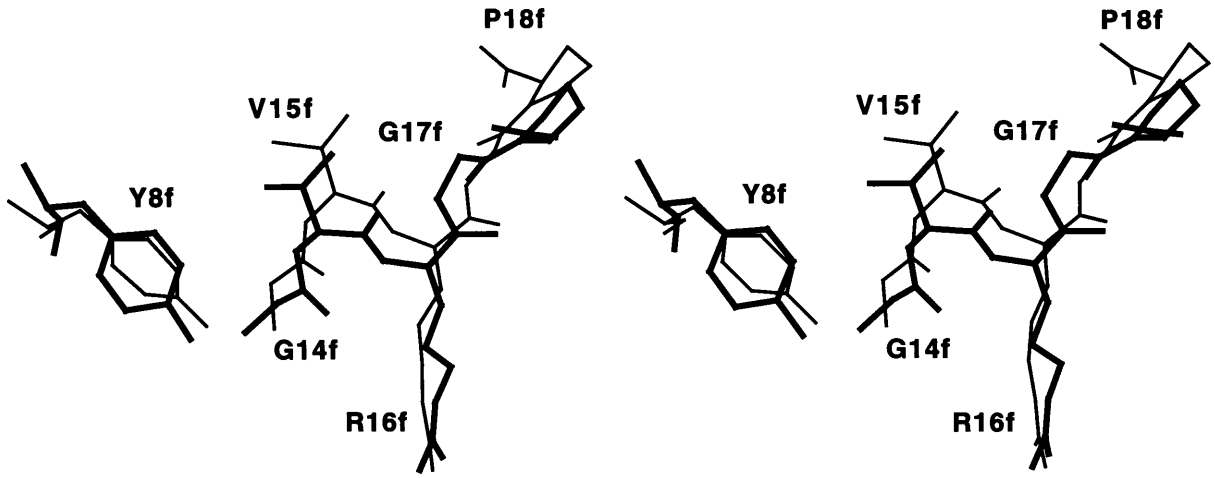

Figure 4 Fibrinopeptide F8Y in complex I and complex II

The F8Y peptide in complex I (thick lines) is compared with F8Y in complex II (thin lines) after the two complexes were overlapped by using only thrombin Cα coordinates.

Table 2 Thrombin interactions with F8Y fibrinopeptides I and II compared with those with the G17ψ substrate analogue

G17ψ-III is complex III in the TBN–G17ψ crystal structure [5]. Note: 1 Å ≡ 0.1 nm.

		Distance (Å)		
Fibrinopeptide atom	Thrombin atom	F8Y-I	F8Y-II	G17ψ-III
Tyr/Phe-8f N	Lys-97 O	2.5	2.7	2.8
	Glu-97A O			3.1
Tyr-8f OH	Gly-14f N	2.2	2.7*	
Gly-14f N	Gly-216 O		2.2	3.0
	Tyr-8f OH	2.2	2.7*	
Gly-14f O	Gly-216 N	2.8		3.1
Arg-16f N	Ser-195 OG	3.1		3.1
	Ser-214 O	3.1		
	Gly-14f O		2.9	
Arg-16f O	Gly-193 N	2.9	3.0	2.8
	Ser-195 N			3.0
Arg-16f NE	Ala-190 O	3.3		
	Gly-219 O		3.2	
Arg-16f NH1	Asp-189 OD2	3.1		2.9
	Trp-215 O		3.2	
Arg-16f NH2	Asp-189 OD1	3.2	2.5	2.9
	Asp-189 OD2	3.1		
	Gly-219 O	2.7	3.0	2.8

* Angle of 83 ° is slightly less than 90 ° limit.

B-chain residues (16–247), and data from the first crystal only. By using XPLOR, the R factor was reduced from 0.406 to 0.362 with 50 cycles of rigid-body refinement and further reduced to 0.236 for data from 7–3.2 Å resolution with 120 cycles of positional refinement. At this point, a $2F_o-F_c$ electron density map allowed us to fit residues Tyr-8f and Gly-14f to Pro-18f of the F8Y fibrinopeptide in both complexes. After 120 additional cycles of positional refinement, the R factor was 0.195 for data from 7–3.2 Å resolution.

Subsequent refinement was done with the merged data from both crystals (7–2.5 Å resolution; $|F_{hkl}| > 2\sigma$). Residues with poorly defined density in a $2F_o-F_c$ electron density map, namely the six N-terminal residues and the C-terminal residue of the A-chain (1H–1C; Arg-15), the autolysis loop (147–149E), and the C-terminus of the B-chain (244–247) were removed before proceeding with further refinement. A total of 276 water molecules were then added at positions that were within 2.5–3.5 Å of a hydrogen bond donor or acceptor and had density in both F_o-F_c and $2F_o-F_c$ maps. Final cycles of positional refinement in GPRLSA [30] and temperature factor refinement in XPLOR decreased the R factor to 0.183 for 2σ data from 7–2.5 Å resolution.

The final refined model of TBN–F8Y had root mean square (RMS) deviations from reference values of 0.015 Å on bonds, 2.48 ° on angles, 1.34 ° on impropers and 24.58 ° on dihedrals. On the Ramachandran plot calculated with PROCHECK [31], 78 % of the residues lay in the most favoured regions (compared with a typical value of 77 % for other structures at 2.5 Å resolution), 21 % in additionally allowed regions and 1 % (five residues) in disallowed regions. The nine other parameters evaluated by PROCHECK were within the bounds established from well-refined structures at equivalent resolution or on the better side of these regions. The average coordinate error [32] of the structure was 0.25–0.30 Å as determined in XPLOR. When the final model was subjected to simulated annealing at 4000 K by using 95 % of the data, R_{free} started at 0.303 and decreased to 0.245 after positional refinement.

Thrombin

The two independent thrombin molecules in complexes I and II include residues 1B–14M of the A-chain, and residues 16–146 and 150–243 of the B-chain. There is no density for the first 13 residues of the A-chain or for the single carbohydrate chain attached to Asn-60G. Residues 1H–1C at the A-chain N-terminus, residue 15 at the A-chain C-terminus, and residues 244–247 at the B-chain C-terminus, have poor density and are not in the model. The autolysis loop, corresponding to residues 145–150 of the thrombin B-chain, has fragmented density and has also been removed. However, the electron density is consistent with complex I's being bovine α-thrombin cut between residues

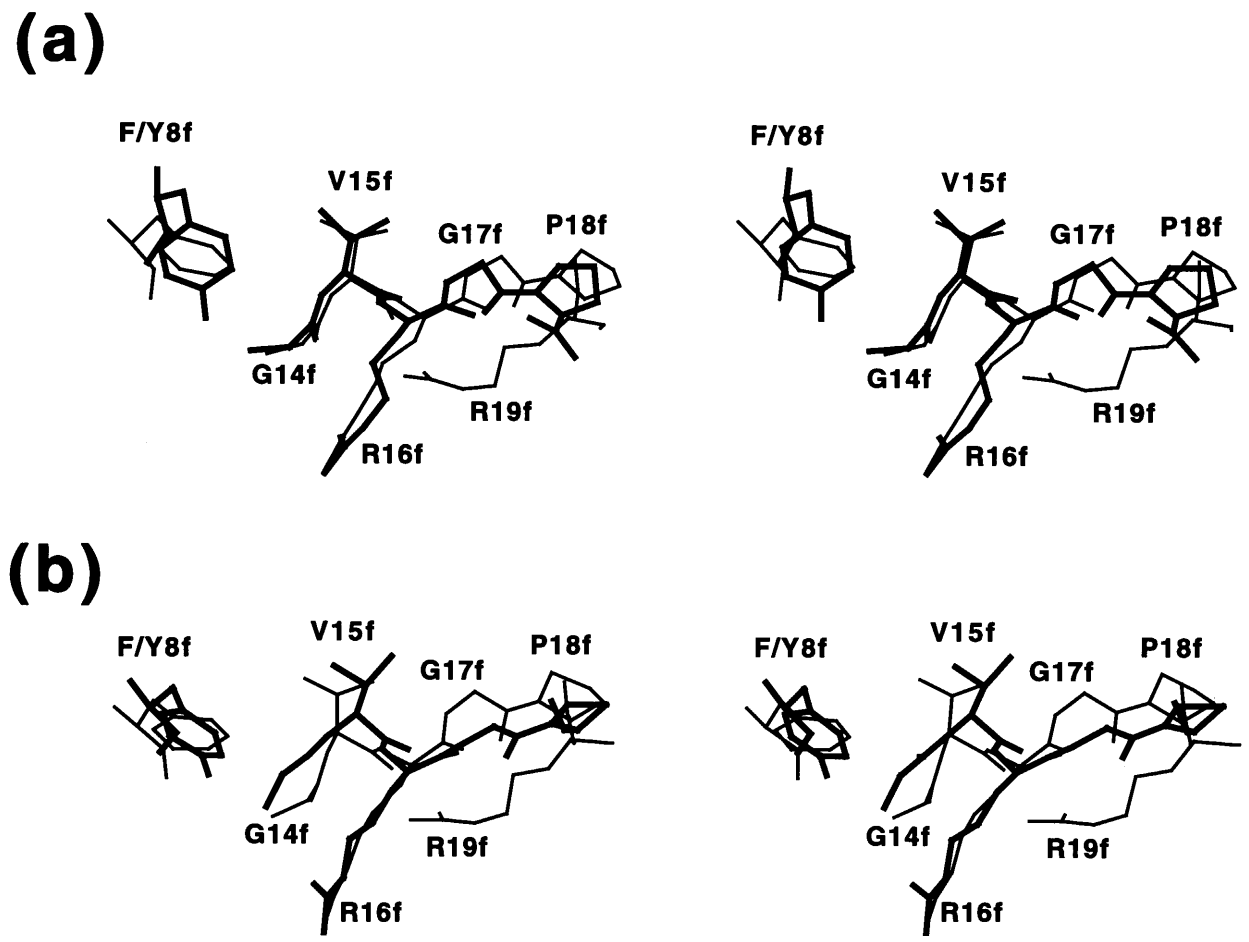

Figure 5 Comparison of F8Y with the non-cleavable substrate analogue G17ψ

Residues 8f and 14f–18f of F8Y (thick lines) are shown in stereo for (**a**) complex I and (**b**) complex II overlapped with the corresponding residues of TBN–G17ψ (thin lines).

Ala-149A and Asn-149B (ϵ-thrombin) and complex II's being α-thrombin in a manner similar to that seen in crystals of TBN–FpA7 and TBN–G17ψ [4,5].

The RMS deviation in Cα coordinates is 0.46 Å when the two complexes are compared together; 0.51 and 0.52 Å respectively when the two complexes are compared against PPACK-thrombin [3]; and 0.46 and 0.46 Å respectively when compared with TBN–FpA7 (complex III in [4]). These deviations indicate that the structures of the two complexes are very close to one another and to other well-refined thrombin structures. A total of 37 residues, in either one or both thrombin molecules, have RMS deviations greater than 1.0 Å at their Cα positions. These deviations are reasonable given that the residues lie at the termini of the A-chain or B-chain, or contact symmetry-related molecules or reside in mobile surface loops as evidenced by temperature factors well above the average values of 15.5 and 22.6 Å^2 for thrombin in complexes I and II respectively.

Fibrinopeptide

There was no electron density for residues 1–7 of the fibrinopeptide, confirming previous published reports that the first six residues of the fibrinopeptide do not interact with thrombin [13,14,33,34]. Well-defined electron density was seen for residue Tyr-8f and for residues Gly-14f to Pro-18f but there was no interpretable density for Leu-9f to Gly-13f (Figures 2 and 3). Instead of following the same path as that seen in TBN–FpA7 and TBN–G17ψ, these five intervening residues form a disordered linker chain through open solvent regions. As a consequence, part of the original path is now occupied by crystal contacts. There was also no electron density for the last five residues of the F8Y peptides, Arg-19f to Arg-23f.

The two F8Y peptides, which had an RMS deviation of 1.1 Å in Cα positions relative to one another (Figure 4), bound in similar but not identical orientations (Table 2). Although Tyr-8f in both F8Y complexes has moved relative to the position of Phe-8f in FpA7 or G17ψ (Figure 5), it still makes the strong hydrogen bond between the backbone NH at position 8f and the carbonyl oxygen of Lys-97 that is present in the TBN–G17ψ and TBN–FpA7 complexes [4,5]. The side chain of Tyr-8f, like that of Phe-8f, lies within the hydrophobic pocket formed by thrombin residues Tyr-60A, Leu-99, Ile-174 and Trp-215 and the side chain of Val-15f. In complex II, Tyr-8f contacts Trp-60D in a symmetry-related molecule as well. This contact is the only packing interaction involving either F8Y peptide. Uniquely to F8Y, the phenol side chain of Tyr-8f forms an intrapeptide hydrogen bond with Gly-14f NH (Table 2).

Perhaps owing to the interaction with Tyr-8f, Gly-14f makes a single hydrogen bond with Gly-216 (Table 2), in contrast with the G17ψ peptide and most other serine protease inhibitors,

which make both possible hydrogen bonds. Val-15f lies between thrombin residues Trp-60D and Leu-99, where its side chain forms part of the hydrophobic cage surrounding Tyr-8f. It has no hydrogen bonds with thrombin (Table 2) but does form an intrapeptide hydrogen bond in complex I with Gly-17f.

In both TBN–F8Y complexes, the side chain of Arg-16f is hydrogen-bonded to Asp-189 and Gly-219 in the specificity pocket. However, in complex I there is also a hydrogen bond with Ala-190 and in complex II a hydrogen bond with Trp-215 (Table 2). Likewise, the main chain of Arg-16f is hydrogen-bonded to Gly-193 in all three complexes, but hydrogen bonds with Ser-214, Ser-195 and Gly-14f are also seen in at least one of the complexes. Gly-17f has no polar interactions with thrombin in the F8Y complexes. Although Pro-18f is in approximately the same S2′ site as in the G17ψ complexes, it is shifted more towards the solvent and is not packed as tightly against the carbonyl oxygens of Leu-40 and Leu-41 (Figure 5).

DISCUSSION

Structure of the thrombin molecules

The two thrombin molecules in the asymmetric unit are crystallographically independent but have almost identical tertiary structures. Residues exhibiting differences larger than 1.0 Å, i.e. more than twice the RMS deviation, are generally located at mobile termini or loops or crystal packing contacts. An exception occurs at the 'YPPW loop', Tyr-60A to Trp-60D, which usually shows little variation between thrombin structures [35]. The loop is well defined in both F8Y complexes, as indicated by the low average B values of 13 and 16 Å^2 respectively, but the two loops have RMS deviations of 0.9 and 1.4 Å respectively relative to TBN–G17ψ, and 1.2 Å relative to each other. The movement maintains the hydrophobic contact seen in previous studies with the side chain of Val-15f [4,5,10], which has a different position in each F8Y complex (Figure 4).

Fibrinopeptide structure and interactions with thrombin

The canonical structure of FpA bound to thrombin consists of a single turn of helix, formed by Asp-7f to Glu-11f, which is linked via Gly-12f and a type I β-bend, involving residues Leu-9f to Gly-12f, to an extended chain of residues Gly-13f to Arg-16f [4,5,10]. Positions for residues Gly-17f to Arg-19f (P1′–P3′) are known from the structure of thrombin complexed with G17ψ, an uncleavable substrate analogue, in which the scissile peptide bond is replaced by a ketone–methylene carbon bond [5]. In TBN–F8Y, Arg-19f to Arg-23f do not have corresponding electron density and are disordered.

In TBN–FpA7 and TBN–G17ψ the turn of helix and the β-bend are stabilized almost exclusively by intrapeptide hydrogen bonds. The only interactions with thrombin, besides the hydrophobic cage around Phe-8f, are a hydrogen bond between the amide nitrogen of Phe-8f and the carbonyl oxygen of Lys-97 and a salt bridge between the side chains of Glu-11f and Arg-173. The next significant interaction with thrombin does not occur until Gly-14f, which makes the antiparallel β-strand hydrogen bonds with Gly-216.

Although the salt bridge does not exist in TBN–F8Y, Glu-11f has no density and the side chain of Arg-173 is rotated away to hydrogen bond with water molecules, Tyr-8f retains most of the hydrophobic interactions and also the main-chain hydrogen bond with Lys-97. However, in both TBN–F8Y complexes the carbonyl oxygen of Tyr-8f, which participates in multiple intrapeptide hydrogen bonds that stablilize the secondary structure in TBN–FpA7 and TBN–G17ψ, has moved by 1.8 Å in both F8Y complexes. Apparently, this large shift weakens the intrapeptide interactions to the point that the helix becomes unstable. Tyr-8f is shifted from the position of Phe-8f because the phenol group is larger and makes a new hydrogen bond with the amide nitrogen of Gly-14f (Table 2). The phenol ring does not retain the edge-to-face stacking with Trp-215 seen for Phe-8f in TBN–FpA7 and TBN–G17ψ.

The peptide secondary structure is also probably disordered or only weakly present in solution. The TBN–F8Y complex, which is crystallized under essentially the same conditions as the TBN–FpA7 and TBN–G17ψ, forms a quite different unit cell in which residues from symmetry-related complexes actually overlap the path that the peptide would follow if it retained the canonical turns. If the peptide turns were as stable in TBN–F8Y as in the other fibrinopeptide complexes, this crystal packing would not be possible.

In the TBN–G17ψ complexes, Gly-17f has only van der Waals contacts, Pro-18f contacts the carbonyl oxygens of Leu-40 and Leu-41, and Arg-19f interacts with Glu-192 in one orientation and Glu-39 in an alternative orientation [5]. However, in TBN–F8Y the carbonyl carbon of Pro-18f is displaced by 1.5 and 2.1 Å respectively towards the solvent in complexes I and II relative to Pro-18f in the G17ψ complex (Figure 5). Consequently, Arg-19f cannot make the same interactions as in the substrate analogue complex and is shifted out into the solvent instead. In agreement with this analysis, the side chains of Glu-39 and Glu-192 have moved away from their positions in the TBN–G17ψ complex.

Val-20f has been postulated to interact with Phe-60H [35]. In the F8Y complexes, Val-20f has no electron density and therefore the proposed interaction with Phe-60H cannot be evaluated. However, the Cα atom of Pro-18f, the last F8Y peptide residue seen in our structure, is 14.7 Å from the Cα atom of Phe-60H. Residues Val-21f to Arg-23f do not increase the specificity constant [18] and therefore are not expected to interact significantly with thrombin; they are probably part of an external loop that links the cleavage site with the sequence that binds at the fibrinogen recognition exosite [35].

Catalytic site

In both complexes the electron density for the scissile bond and for residues Gly-17f and Pro-18f is well defined and continuous in the $2F_o-F_c$ 'omit' electron density maps calculated in XPLOR (Figure 3). However, the overall temperature factors for F8Y in complexes I and II are 53.1 and 59.9 Å^2 respectively, almost three times the average overall temperature factor for the entire structure (22.3 Å^2). These elevated B values for F8Y are probably due to some combination of higher mobility, partial occupancy or partial cleavage of F8Y. The electron density in the unbiased 'omit' map (Figure 3) shows that a significant portion of the F8Y peptide in both crystallographically independent complexes is uncleaved. However, hydrolysis does continue slowly. Mass spectrometric analysis on 14 dissolved TBN–F8Y crystals that were harvested from drops equilibrated for 21 days showed a peak for FpA at 1554 Da but no peaks at higher molecular masses. When the crystal structure was refined as a cleaved, product complex, Gly-17 and Pro-18 did not fit the electron density (results not shown). Moreover, if F8Y were fully cleaved, the P′1 and P′2 residues, which have limited interactions with thrombin, would not be present, as shown by the structure of TBN–FpA7 [9]. In these crystals, which are grown under conditions similar to those used for F8Y, there is no electron density for residues beyond Arg-16f, although the FpA7 peptide was synthesized as Asp-7f to Asp-20f. The FpA7 peptide is

Table 3 Ramachandran angles for P3 to P′3

Canonical angles are from [38]. Angles in parentheses are outside the canonical range.

	Angle (degrees)							
	Canonical limits		G17ψ-III		F8Y-I		F8Y-II	
Position	ϕ	ψ	ϕ	ψ	ϕ	ψ	ϕ	ψ
P3 G14f	−120/−140	140–170	−136	(122)	–	(113)	–	(−159)
P2 V15f	−60/−100	139–180	−68	157	(−59)	(105)	−75	(92)
P1 R16f	−95/−120	9–50	−101	29	(−59)	19	(−78)	(66)
P′1 G17f	−60/−100	139–180	−74	166	−68	151	(−145)	173
P′2 P18f	−99/−140	70–120	−70	132	(−41)	(176)	(−39)	119
P′3 R19f	−99/−140	70–120	−102	(3)	–	–	–	–

Table 4 Active site geometry

	Angle (degrees)			Distance (Å)
Complex	Oγ ⋯ C–O*	Oγ ⋯ C–Ca	Oγ ⋯ C–N	Oγ ⋯ C
Optimum*	90	90	90	
G17ψ-III†	90	92	85	2.6
F8Y-I	88	84	99	2.4
F8Y-II	64	82	134	3.8‡
Ovomucoid	95	84	97	2.7

* From [36].

† The angles and distances are measured from the Oγ of Ser-195 to the substrate atoms.

‡ Ser-195 Oγ and carbonyl carbon atom of F8Y-II are both displaced by 0.7 Å from the positions in the G17ψ substrate analogue. The distance from Ser-195 Oγ in F8Y-II to the carbonyl carbon in the overlapped substrate analogue (i.e. the ideal position) is 3.1 Å.

rapidly cleaved at Arg-16f during crystallization and the last four residues do not bind to thrombin [4].

Because the peptide secondary structure is disordered, F8Y binds at the catalytic site with torsion angles that differ significantly from the canonical values and from the values of the G17ψ substrate analogue (Table 3). As a consequence, the F8Y peptides in complexes I and II have RMS deviations of 1.1 and 0.9 Å respectively when compared with the substrate analogue (Figure 5) and have distorted catalytic geometry (Table 4).

Although the F8Y peptide has a susceptible Arg-16f–Gly-17f bond and is bound to active thrombin, as evidenced by catalytically appropriate hydrogen bonds between Ser-195, His-57 and Asp-102 (2.5–2.8 Å), the peptide is cleaved at a much lower rate because F8Y binds with geometry that is incompatible with nucleophilic attack by Ser-195 on the carbonyl carbon. Theoretical calculations show that the reaction proceeds optimally when the serine hydroxy oxygen, carbonyl carbon and carbonyl oxygen make a right-angled triangle (angle OG ⋯ C═O of 90 °) that is perpendicular to the plane of the scissile peptide bond [36]. The substrate analogue, G17ψ, binds almost exactly in this fashion (Table 4). In contrast, F8Y is a very poor substrate because it binds with a reaction geometry that is non-ideal, like a natural peptide inhibitor such as turkey ovomucoid bound to trypsin (Table 4). Thus the interaction of Phe-8f with the apolar site in thrombin is critical for the proper orientation of the scissile bond and efficient nucleophilic attack by Ser-195.

Received 3 February 1997/16 May 1997; accepted 23 May 1997

This work was supported by National Institutes of Health grants HL57527 (B. F. P. E.) and HL45100 (S. T. L.) and a training fellowship to M. G. M. from NIH grant T32 HL07602.

REFERENCES

1 Davie, E. W., Fujikawa, K. and Kisiel, W. (1991) Biochemistry **30**, 10363–10370
2 Fenton, J. W. I. I. (1988) Semin. Thromb. Hemostasis **14**, 234–240
3 Bode, W., Mayr, I., Baumann, U., Huber, R., Stone, S. R. and Hofsteenge, J. (1989) EMBO J. **8**, 3467–3475
4 Martin, P. D., Robertson, W. D., Turk, D., Huber, R., Bode, W. and Edwards, B. F. P. (1992) J. Biol. Chem. **267**, 7911–7920
5 Martin, P. D., Malkowski, M. G., DiMaio, J., Konishi, Y., Ni, F. and Edwards, B. F. P. (1996) Biochemistry **35**, 13030–13039
6 Vitali, J. V., Martin, P. D., Malkowski, M. G., Robertson, W. D., Lazar, J. B., Winant, R. C., Johnson, P. H. and Edwards, B. F. P. (1992) J. Biol. Chem. **267**, 17670–17678
7 Brandstetter, H., Turk, D., Hoeffken, H. W., Grosse, D., Stürzebecher, J., Martin, P. D., Edwards, B. F. P. and Bode, W. (1992) J. Mol. Biol. **226**, 1085–1099
8 Rydel, T. J., Ravichandran, K. G., Tulinsky, A., Bode, W., Huber, R. and Roitsch, C. (1990) Science **249**, 277–283
9 Grütter, M. G., Priestle, J. P., Rahuel, J., Grossenbacher, H., Bode, W., Hofsteenge, J. and Stone, S. R. (1990) EMBO J. **9**, 2361–2365
10 Stubbs, M. T. and Bode, W. (1992) Eur. J. Biochem. **206**, 187–195
11 Fenton, J. W. I. I., Olson, T. A., Zabinski, M. P. and Wilner, G. D. (1988) Biochemistry **27**, 7106–7112
12 Lord, S. T., Byrd, P. A., Hede, K. L., Wei, C. and Colby, T. J. (1990) J. Biol. Chem. **265**, 838–843
13 Blombäck, B. (1986) Ann. N. Y. Acad. Sci. **485**, 120–123
14 Scheraga, H. A. (1986) Ann. N. Y. Acad. Sci. **485**, 124–133
15 Binnie, C. G. and Lord, S. T. (1993) Blood **81**, 3186–3192
16 Marsh, H. C. J., Meinwald, Y. C., Lee, S. and Scheraga, H. A. (1982) Biochemistry **21**, 6167–6174
17 Ni, F., Meinwald, Y. C., Vasquez, M. and Scheraga, H. A. (1989) Biochemistry **28**, 3094–3105
18 Marsh, H. C. J., Meinwald, Y. C., Thannhauser, T. W. and Scheraga, H. A. (1983) Biochemistry **22**, 4170–4174
19 Martin, P. D., Kumar, V. K., Tsernoglou, D. and Edwards, B. F. P. (1983) Fed. Proc. **42**, 1861–1861
20 Haverkate, F., Koopman, J., Kluft, C., D'Angelo, A., Cattaneo, M. and Mannuccri, P. M. (1986) Thromb. Haemostasis **55**, 131–135
21 Chambers, J. L., Ortega, R. B. and Campana, C. F. (1992) Abstr. Annu. Meet. Am. Crystallogr. Assoc. 50th **20**, 87
22 Howard, A. J., Gilliland, G. L., Finzel, B. C., Poulos, T. L., Ohlendorf, D. H. and Salemme, F. R. (1987) J. Appl. Crystallogr. **20**, 383–387
23 Reeke, G. N. (1984) J. Appl. Crystallogr. **17**, 125–130
24 Brünger, A. T. (1988) J. Mol. Biol. **203**, 803–816
25 Zhang, K. Y. J. (1993) Acta Crystallogr. **D49**, 213–222
26 Vitali, J., Martin, P. D., Malkowski, M. G., Olsen, C. M., Johnson, P. H. and Edwards, B. F. P. (1996) Acta Crystallogr. **D52**, 453–464
27 Bernstein, F. C., Koetzle, T. F., Williams, G. J. B., Meyer, E. F. J., Brice, M. D., Rodgers, J. R., Kennard, O., Shimanouchi, T. and Tasumi, M. (1977) J. Mol. Biol. **112**, 535–542
28 Baker, E. N. and Hubbard, R. E. (1984) Prog. Biophys. Mol. Biol. **44**, 97–179
29 Satow, Y., Cohen, G. H., Padlan, E. A. and Davies, D. R. (1986) J. Mol. Biol. **190**, 593–604
30 Furey, W., Wang, B. C. and Sax, M. (1982) J. Appl. Crystallogr. **15**, 160–166
31 Laskowski, R. A., MacArthur, M. W., Moss, D. S. and Thornton, J. M. (1993) J. Appl. Crystallogr. **26**, 283–291
32 Luzatti, P. V. (1952) Acta Crystallogr. **5**, 802–810
33 Henschen, A., Lottspeich, F., Kehl, M. and Southan, C. (1983) Ann. N. Y. Acad. Sci. **408**, 28–43
34 Ménaché, D. (1983) Ann. N.Y. Acad. Sci. **408**, 121–129
35 Stubbs, M. T. and Bode, W. (1993) Thromb. Res. **69**, 1–58
36 Klebe, G. (1991) in The Application of Charge Density Research to Chemistry and Drug Design, Correlation of Crystal Data and Charge Density with the Reactivity and Activity of Molecules: Towards a Description of Elementary Steps in Enzyme Reactions (Jeffrey, G. A. and Pinella, J. F., eds.), pp. 287–318, Plenum Press, New York
37 Schechter, J. and Berger, A. (1967) Biochem. Biophys. Res. Commun. **27**, 157–162
38 Bode, W. and Huber, R. (1992) Eur. J. Biochem. **204**, 433–451